

Giant anharmonicity and non-linear electron-phonon coupling in MgB₂; Combined first-principles calculations and neutron scattering study

T. Yildirim⁽¹⁾, O. Gülseren^(1,2), J. W. Lynn⁽¹⁾, C. M. Brown^(1,3), T. J. Udovic⁽¹⁾, H. Z. Qing^(1,3), N. Rogado⁽⁴⁾, K.A. Regan⁽⁴⁾, M.A. Hayward⁽⁴⁾, J.S. Slusky⁽⁴⁾, T. He⁽⁴⁾, M.K. Haas⁽⁴⁾, P. Khalifah⁽⁴⁾, K. Inumaru⁽⁴⁾, and R.J. Cava⁽⁴⁾

⁽¹⁾ NIST Center for Neutron Research, National Institute of Standards and Technology, Gaithersburg, MD 20899

⁽²⁾ Department of Materials Science and Engineering, University of Pennsylvania, Philadelphia, PA 19104

⁽³⁾ University of Maryland, College Park, MD

⁽⁴⁾ Department of Chemistry and Princeton Materials Institute, Princeton University, Princeton, NJ 08544

(July 13, 2021)

We report first-principles calculations of the electronic band structure and lattice dynamics for the new superconductor MgB₂. The excellent agreement between theory and our inelastic neutron scattering measurements of the phonon density of states gives confidence that the calculations provide a sound description of the physical properties of the system. The numerical results reveal that the in-plane boron phonons (with E_{2g} symmetry) near the zone-center are very anharmonic, and are strongly coupled to the partially occupied planar B σ bands near the Fermi level. This giant anharmonicity and non-linear electron-phonon coupling is key to quantitatively explaining the observed high T_c and boron isotope effect in MgB₂.

PACS numbers: 63.20.Ry, 63.20.Kr, 61.12.-q, 74.25.Jb, 74.25.Kc

The recent discovery of superconductivity at 40 K in the MgB₂ binary alloy system [1] has triggered enormous interest in the structural and electronic properties of this class of materials. The system has a very simple crystal structure [2], where the boron atoms form graphite-like sheets separated by hexagonal layers of Mg atoms (see inset to Fig. 1). Our pseudopotential plane wave band structure calculations show that the bands near the Fermi level arise mainly from the $p_{x,y}$ σ bonding orbitals of boron, while the Mg does not contribute appreciably to the conductivity, in good agreement with initial reports from other groups [3–5]. In the case of graphite these σ bands are full, but for MgB₂ they are partially unoccupied, creating a hole-type [6] conduction band like the high-T_c cuprates. In contrast to the cuprates, however, the normal-state conductivity is three-dimensional in nature instead of being highly anisotropic, thus eliminating the “weak-link” problem that has plagued widespread commercialization of the cuprates. The normal-state conductivity [6–8] is also one to two orders-of-magnitude higher than either the Nb-based alloys or Bi-based cuprates used in present day wires, and this feature combined with low cost and easy fabrication [8,9] could make this class of materials quite attractive for applications.

From a fundamental point of view the central question is whether the high T_c in this new system can be understood within the framework of a conventional electron-phonon mechanism, or a more exotic mechanism is responsible for the superconducting pairing. The observed boron isotope effect [10] argues for an electron-phonon mechanism, while the positive Hall coefficient [6] suggests similarities with the cuprates [11]. To answer this question, we have carried out inelastic neutron scattering measurements of the phonon density of states, and compare these results with detailed first-principles calcu-

lations of the lattice dynamics (and electronic) calculations for MgB₂. Excellent agreement is found between theory and experiment. More importantly, the numerical results demonstrate that the in-plane boron phonons near the zone-center (with E_{2g} symmetry at Γ) are very anharmonic and strongly coupled to the partially occupied conduction band (planar B σ bands) near the Fermi level, providing the large electron-phonon interaction in this system. Due to these strong anharmonic phonon modes, the electron-phonon coupling is non-linear, providing the essential ingredient to explain the high T_c and boron isotope effect in MgB₂.

The results of the neutron measurements and calculations for the phonon density of states are summarized in Fig. 1. For the experimental data, the 5g polycrystalline sample was prepared in the usual way with the ¹¹B isotope to avoid neutron absorption problems [12], and was characterized by magnetization, x-ray, and neutron diffraction. Inelastic neutron scattering measurements were made to determine the generalized phonon density of states (GPDOS), which is the phonon density of states weighted by the cross section divided by the mass of each atom. The data were collected from 7 K to 325 K on the Filter Analyzer Spectrometer in the range 5-130 meV, and on the Fermi chopper instrument for energies of 0.5-30 meV. Additional details of the experiment and analysis can be found elsewhere [13,14]. The experimental data indicate two bands of phonons, one below 40 meV corresponding primarily to the acoustic phonon modes, and one above 50 meV that mostly involves the boron motions. The high-energy portion of the spectrum shows a sharp cutoff at about 100 meV. The data are in basic agreement with the results of Osborn *et al.* [15], although the present data were obtained with better overall energy resolution. Our results do not agree with Sato *et al.* [16], who reported a feature at 17 meV in the GPDOS. We did

not observe this feature at any temperature and conclude that it is not intrinsic to the GPDOS. We also have measured the temperature dependence of the spectrum and find no substantial changes in the basic features from 7 K up to 200 K, while a very modest softening of some of the modes was observed in going to 325 K.

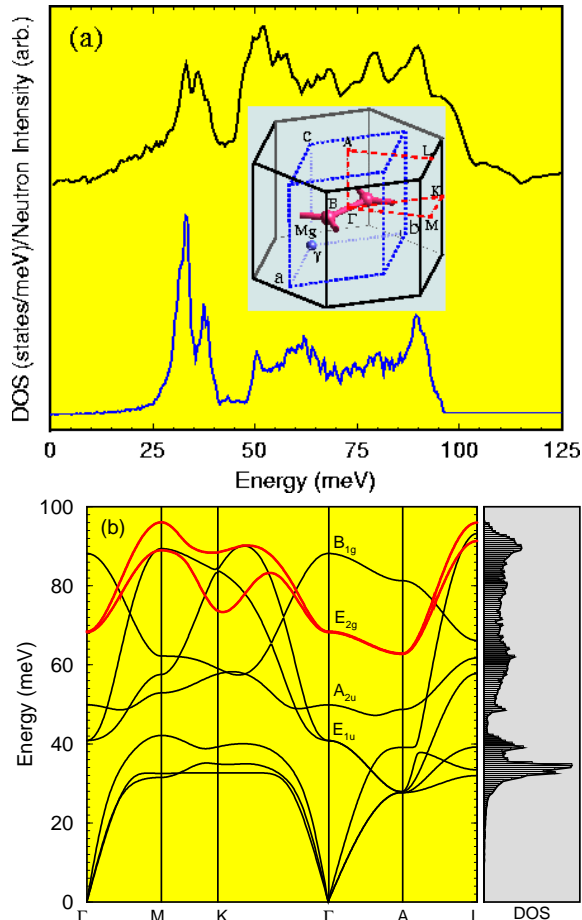


Fig. 1 (a) Generalized phonon density of states for MgB₂ (top curve) determined from inelastic neutron scattering measurements, and the calculated phonon density of states (DOS) (bottom curve). The inset shows the unit cell of MgB₂ along with the Brillouin zone and the high-symmetry directions. (b) Calculated dispersion curves of all phonons and the corresponding DOS (right panel). At the zone center (Γ), the symmetries of the modes are also indicated. The modes indicated by the red-line dominate the electron-phonon coupling.

In order to understand the origin of the features observed in the neutron data, we have carried out detailed first-principles calculations of the electronic band structure and lattice dynamics. The calculations were performed using the pseudopotential plane wave method [17], within the generalized gradient approximation [18]. We employed plane waves with an energy cutoff of 500 eV, and the ultra-soft pseudopotentials for Mg and B [19]. The total energy and forces converged within 0.5 meV/atom and 0.01 eV/Å, respectively. Brillouin-zone

integrations [20] were carried out using $dk = 0.02 \text{ \AA}^{-1}$, generating $15 \times 15 \times 11$ and $9 \times 9 \times 6$ k-points for $1 \times 1 \times 1$ and $2 \times 2 \times 2$ supercells, respectively. The lattice parameters a and c were relaxed before the lattice dynamics calculations, and the force constant matrix was obtained by the direct-force method using periodically repeated supercells [23]. The optimized lattice parameters are in good agreement with our experimental values within 1%. The calculated density of states obtained from these calculations is shown in Fig. 1a, and we see that the agreement between experiment and theory for the energies of the modes is excellent. The agreement for the intensities is also good considering that the observed spectrum is a weighted density of states rather than the actual DOS, and the wave vector averaging may include some coherency effects [13]. The calculated phonon dispersion curves along the high-symmetry directions of the Brillouin-zone (see inset to Fig. 1) are shown in Fig. 1b. All the modes are found to be quite dispersive as expected for the small size of the unit cell, but divide nearly completely into acoustic (below ≈ 40 meV) and optical (50-100 meV) bands, with the only exception being along the A-L direction. All the optical modes are weakly dispersive along the Γ -A direction, reflecting the layered nature of the MgB₂ crystal structure.

There are four distinct phonon modes at the zone center Γ , as indicated in Fig. 1b. The A_{2u} and B_{1g} singly-degenerate modes involve only vibrations along the c axis; for B_{1g} the boron atoms move in opposite directions while the Mg ion is stationary, while for the A_{2u} mode the Mg and B planes move in opposite directions along the z -axis. The other two modes are doubly degenerate and involve only in-plane motions (along the x or y axes). For the E_{1u} mode the Mg and B planes vibrate in opposite directions along the x (or y) axis. The calculated energies of all zone-center phonons are listed in Fig. 2, and for the three types of modes just discussed there is good agreement between calculations reported by other groups [3–5]. For the E_{2g} mode, however, there are large discrepancies between the results reported for various calculations. The boron ions for this mode vibrate in opposite directions along the x (or y) axis, with the Mg ions stationary. The discrepancies noted above are resolved when the strong anharmonicity associated with the in-plane displacements of the boron atoms is taken into account.

To further investigate this behavior, we plot in Fig. 2 the energy as the atoms are displaced by an amount u according to each of the four eigenmodes. For the B_{1g} , A_{1u} , and E_{1u} modes the distortion energy can be very well approximated by the harmonic expression $E(u) = A_2 u^2$ up to $u/a = 0.065$. It is unusual that the phonons remain harmonic at these large distortions, but this is consistent with the fact that we did not observe any substantial changes in the measured GPDOS with temperature.

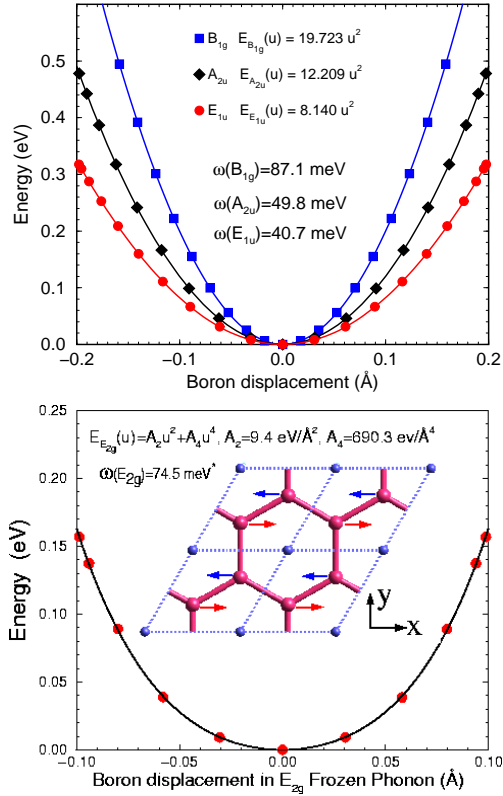


Fig. 2 Energy curves as a function of boron displacement for each zone center frozen-phonon mode. The top panel shows that the B_{1g} , A_{2u} , and E_{1u} modes are harmonic up to $u/a \approx 0.065$. The bottom panel shows that the E_{2g} boron in-plane mode is very anharmonic. The inset indicates one of the E_{2g} modes. Animations of these modes and their coupling with the electronic structure can be found at <http://www.ncnr.nist.gov/staff/taner/mgb2>.

The most interesting observation, though, is the totally opposite behavior of the E_{2g} in-plane boron mode, as shown in Fig. 2b. The potential well is very shallow at small displacements and increases rapidly at large displacements, and can be fit very well to $E(u) = A_2 u^2 + A_4 u^4$ with a large ratio of $A_4/A_2^2 \approx 8$. This indicates that this mode is unusually anharmonic and that we are in a non-perturbative regime. Hence the estimated harmonic energy, $\omega_H(E_{2g}) = 60.3$ meV will be lower than the actual energy. Using Hartree-Fock decoupling, one gets $E(u) = (A^2 + 3A_4 \langle u^2 \rangle) u^2$, where $\langle u^2 \rangle = /2M\omega_{sch}$ and ω_{sch} is the Self Consistent Harmonic (SCH) [22] solution of $\omega_{sch}^2 = [(A_2 + 3A_4 \langle u^2 \rangle)/M]^{1/2}$. This yields a better estimate of $\omega_{sch} \approx 70$ meV, a 17% enhancement of the harmonic phonon energy $\omega_H(E_{2g})$. We can calculate the *exact* energy levels of the potential by numerically solving the Schrodinger equation and obtain $\omega(E_{2g}) = 74.5$ meV, a 25% enhancement of the harmonic value and also the T_C , which then matches with the peak in the GPDOS.

Since the in-plane motions of the boron will change the boron orbital overlap, significant electron-phonon cou-

pling can be expected for the planer σ boron conduction band at the Fermi level and this plays an important role in the superconducting pairing. This can be most easily seen by comparing the band structure of the undistorted lattice to that of distorted one by a zone center phonon. For the harmonic phonons we did not see any significant changes near the Fermi level. However, for E_{2g} modes, there is a significant splitting of the bands as well as shifts near the Fermi level as shown in Fig. 3, indicating strong electron-phonon coupling.

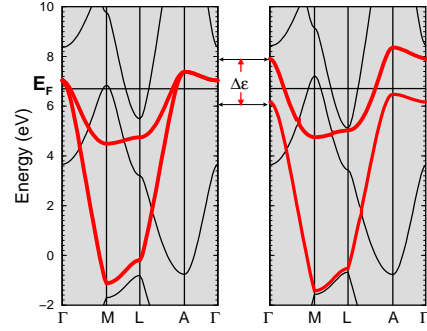


Fig. 3 Band structure of the undistorted (left) and distorted structures (right) by E_{2g} phonons ($u_B \approx 0.06\text{\AA}$). Band structure of the other three frozen-phonon structures do not show any significant changes.

To determine the electron-phonon (EP) coupling quantitatively, we evaluated the Fermi-surface averaged deformation potential,

$$\Delta = \langle [\delta\epsilon(\mathbf{k}) - \delta\mu]^2 \rangle, \quad (1)$$

for each zone-center frozen phonon [23]. Here $\delta\epsilon(\mathbf{k})$ is the change in the one-particle energy with momentum \mathbf{k} due to the frozen phonon, $\delta\mu$ the corresponding change in the chemical potential. $\langle \rangle$ denotes an average of \mathbf{k} over the Fermi surface, which we have carried out numerically.

For the harmonic B_{1g} , A_{2u} , and E_{1u} phonons we calculated an insignificant coupling, and conclude that the electron-phonon coupling is negligible for these modes. For the E_{2g} modes, Fig. 4a shows that the coupling $\Delta(u)$ is large and has both quadratic and quartic terms in frozen-phonon amplitude, u , indicating significant non-linear electron-phonon coupling. Neglecting non-linear cross terms, the electron-phonon coupling constant λ for our anharmonic phonon is approximately given by [17]

$$\lambda = N(E_F) \left(B_2' \sum_n \frac{|\langle n|Q|0\rangle|^2}{E_n - E_0} + B_4' \sum_n \frac{|\langle n|Q^2|0\rangle|^2}{E_n - E_0} \right), \quad (2)$$

where $N(E_F)$ is the total density of states at the Fermi energy and equal to 0.69 states/eV/cell. E_n and $|n\rangle$ are the eigenvalues and eigenfunctions of the oscillator E_{2g} in its adiabatic potential shown in Fig. 2b. B_2' and B_4'

are the first and second-order EP coupling, respectively, and obtained from expansion of $\Delta(u)$. Q is the normal coordinate which is related to boron displacement u via a normalization constant. We calculate a total electron-phonon coupling $\lambda = 0.907(0.922)$ for $M_B=10$ (11). Using the McMillan expression for T_C [25] and taking a typical value for $\mu^* = 0.15$, we obtain a T_C of 39.4 K and 38.6 K for $M_B=10$ and $M_B=11$, respectively, yielding an isotope effect $\alpha = 0.21$ [26] (see Fig. 4b). These estimates are in excellent agreement with experiments. Within the above approximation [24], the non-linear EP coupling increases T_C by about 10%. Our preliminary calculations of λ including other non zone-center phonons indicates that the numbers will not change significantly. Therefore we conclude that MgB_2 is a conventional electron-phonon superconductor in the strong-coupling regime.

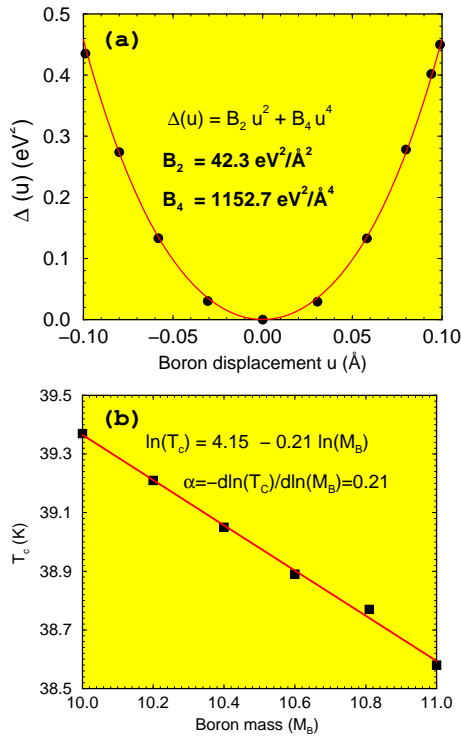


Fig. 4 (a) Calculated Fermi-surface averaged deformation potential $\Delta(u)$. The large quartic term indicates significant non-linear electron-phonon coupling. (b) T_c versus boron mass, indicating a boron isotope effect $\alpha = 0.21$, significantly reduced from harmonic BCS value of 0.5 due to giant anharmonicity [26]. Within our theory, we expect zero isotope effect for Mg, in good agreement with recent report of $\alpha_{Mg}=0.02$ [27].

It is interesting to note that there seems to be a close correlation between the anharmonicity of the E_{2g} in-plane modes and the B-B bond length (d_{BB}). For MgB_2 , d_{BB} is 1.764 Å, significantly stretched from its optimal value of 1.65 Å in elemental planar boron, probably due to repulsive interactions between the Mg and B ions. This explains the unusual anharmonicity and observed

high T_C in MgB_2 . For hypothetical CaB_2 , the calculated d_{BB} is quite large (1.84 Å) and we calculate very large anharmonicity, which may explain the instability of CaB_2 . It then appears likely that MgB_2 is fortuitously just at the phase boundary. It will be interesting to see if it is possible to expand the d_{BB} in MgB_2 by Ca substitution on the Mg site to increase T_C further.

NOTE ADDED IN PROOF: After submission of our work, a recent Raman study [28] has reported 77 meV for the E_{2g} mode with a very large width, confirming our predictions.

ACKNOWLEDGEMENTS: We acknowledge many useful discussion with R. L. Cappelletti and D. A. Neumann.

-
- [1] J. Nagamatsu, N. Nakagawa, T. Muranaka, Y. Zenitani and J. Akimitsu, *Nature* **410**, 63 (2001).
 - [2] M. Jones and R. Marsh, *J. Am. Chem. Soc.* **76**, 1434 (1954).
 - [3] J. Kortus *et al.*, *con-mat/0101446* (2001).
 - [4] J. M. An and W. E. Pickett, *cond-mat/0102391* (2001).
 - [5] Y. Kong *et al.*, *cond-mat/0102499* (2001).
 - [6] W. N. Kang *et al.*, *cond-mat/0102313* (2001).
 - [7] C. U. Jung *et al.*, *con-mat/0102215* (2001).
 - [8] P. C. Canfield *et al.*, *Phys. Rev. Lett.* **86**, 2423 (2001).
 - [9] R. J. Cava, *Nature* **410**, 23 (2001).
 - [10] S. L. Bud'ko *et al.*, *Phys. Rev. Lett.* **86**, 1877 (2001).
 - [11] J. E. Hirsch (*con-mat/0102115*).
 - [12] J. S. Slusky *et al.*, *Nature* **410**, 343 (2001).
 - [13] J. W. Lynn, I. W. Sumarlin, D. A. Neumann, J. J. Rush, J. L. Peng, and Z. Y. Li, *Phys. Rev. Lett.* **66**, 919 (1991).
 - [14] Instrumental details are available at <http://www.ncnr.nist.gov>
 - [15] R. Osborn, E. A. Goremychkin, A. I. Kolesnikov, and D. G. Hinks (*con-mat/0103064*).
 - [16] T. J. Sato, K. Shibata, and Y. Takano (*con-mat/0102468*).
 - [17] M. C. Payne, *et al.*, *Rev. Mod. Phys.* **64**, 1045 (1992).
 - [18] J. P. Perdew and Y. Wang, *Phys. Rev. B* **46**, 6671 (1992).
 - [19] D. Vanderbilt, *Phys. Rev. B* **41**, 7892 (1990).
 - [20] H. J. Monkhorst and J. D. Pack, *Phys. Rev. B* **13**, 5188 (1976).
 - [21] G. Kresse, J. Furthmuller, and J. Hafner, *Europhys. Lett.* **32**, 729 (1995).
 - [22] *Phonons in Perfect Lattices and in Lattices with Point Imperfections*, Ed. by R. W. H. Stevenson (Plenum Press, New York, 1966).
 - [23] F. S. Khan and P. B. Allen, *Phys. Rev. B* **29**, 3341 (1984).
 - [24] V. H. Crespi and M. L. Cohen, *Phys. Rev. B* **48**, 398 (1993).
 - [25] W. L. McMillan, *Phys. Rev.* **167**, 331 (1968).
 - [26] Effect of μ^* and other parameters on the isotope effect will be discussed in T. Yildirim and O. Gulseren, *Phys. Rev. B* (to be published).

- [27] D. G. Hinks, H. Claus, and J. D. Jorgensen, cond-mat/0104242 (2001).
- [28] A. F. Goncharov *et al.*, cond-mat/0104042 (2001).